Classification and analysis of impact on small-signal dynamics and stability from expansion of VSC-HVDC systems to multi-terminal HVDC grids

S. D'Arco, J. Beerten†, J. A. Suul*,#*

*SINTEF Energy Research, 7465 Trondheim, Norway, salvatore.darco@sintef.no
†Department of Electrical Engineering (ESAT), Division ELECTA, University of Leuven (KU Leuven) & Energyville, Belgium
#Department of Electric Power Engineering, Norwegian University of Science and Technology, 7495 Trondheim, Norway,

Keywords: Eigenvalue analysis, HVDC transmission, Modular Multilevel Converters, Small-signal stability, State-space Modelling

Abstract

This paper presents a structured approach for analysing the effect of HVDC transmission system expansion on the small signal dynamics. The methodology decomposes the expansion of the system into a sequence of steps and aims especially at identifying the eigenvalues associated with interactions between the initial system and an added converter terminal. The procedure is illustrated with an example of expanding a point-to-point HVDC connection to a three-terminal radial configuration. The modes highlighted as responsible for the interactions between the initial system and the added third terminal are compared to the interaction modes identified by participation factor analysis. The presented results demonstrate that these two approaches present an excellent correlation and reveal complementary information.

1 Introduction

High Voltage dc (HVDC) transmission systems based on Voltage Source Converters (VSC) are emerging as a viable option for large-scale power transfer and cross-border system integration [1], [2]. VSC technology is also enabling the development of Multi-Terminal dc (MTDC) grids [3]. However, large-scale MTDC grids will likely evolve by extending point-to-point connections and by the merging of smaller MT-HVDC systems [4]-[6]. Thus, it is of critical importance to ensure interoperability and stable operation of the interconnected system in case of gradual expansion of an MTDC grid.

Small-signal stability of large-scale power systems is traditionally studied by eigenvalue analysis. Such analysis can reveal valuable information about the dynamic properties of a system, including how the individual state variables participate in each dynamic mode and the sensitivity of each mode to the various parameters in the system [7]. Several small-signal studies for MT-HVDC systems have been presented during the last years, demonstrating that MT-HVDC systems can present stable operation for a wide range of conditions [8]-[11]. Such studies normally consider a given power system configuration, and potential issues related to system expansion are typically assessed by comparing the behaviour before and after the addition of HVDC terminals.

To support the comparative analysis of small-signal stability studies, as well as investigations of large signal transients and protection issues, a large-scale MTDC test system has been presented by Cigré [12]. In, [13], this test system was used to analyse the effects of a gradual system expansion. This study demonstrated that stability could be ensured when an HVDC system is expanded by adding interconnections and converter terminals. Furthermore, the results indicated that expansion of the system mainly led to additional eigenvalues in similar locations as for the smaller systems. Although this type of analysis can be utilized to identify instabilities or poorly damped oscillatory modes, it does not directly provide clear indications on how potential problems originate from the interconnection of the subsystems.

This paper presents a structured approach for identifying the impact of expanding an HVDC transmission system by adding converter terminals or cable connections. This approach allows for attributing the changes in small-signal dynamics resulting from the system expansion to the following causes:

1) *Changes of equivalent system parameters:* accounting for either changes of controller parameters for accommodating the interconnection, or changes of equivalent physical parameters due to the electrical interconnection.
2) *Change of steady state operating conditions:* accounting for the influence of the non-linearity of the system on the eigenvalues when the system is forced into another operating point.
3) *Dynamic interaction between the different elements of the system:* accounting for the changes of the eigenvalues that result only from the dynamic coupling between two defined sub-systems.

By separating the change of the eigenvalue positions associated to the two first causes from the third, the influence of interactions within the system can be separately identified. For further understanding the impact of connecting two different sub-systems on the eigenvalues of the overall system, the results from the presented analysis are evaluated

This is the accepted version of a paper published in 13th IET International Conference on AC and DC Power Transmission - ACDC 2017
DOI: 10.1049/cp.2017.0050

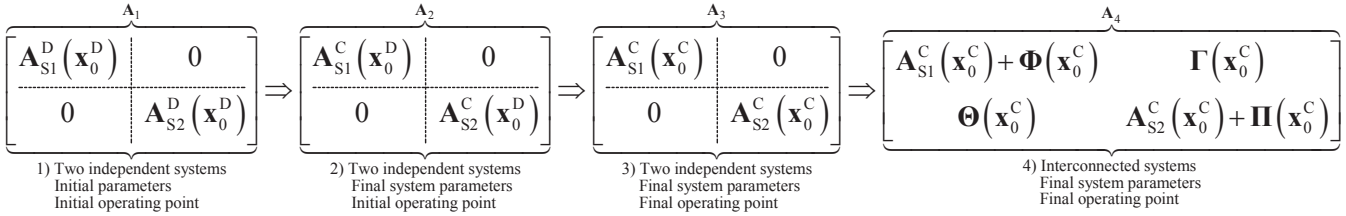

Fig. 1. Illustration of step-wise analysis of the **A**-matrix representing the small-signal dynamics of two systems to be interconnected

with respect to the method for identification of interaction modes in VSC HVDC systems based on aggregated participation factors presented in [14]. The results indicate that the system eigenvalues that can be identified by the proposed approach as associated with the system interactions are coinciding with the interaction modes identified according to the definition proposed in [14]. Thus, the presented analysis is contributing to the understanding of how the impact of system expansion on small-signal dynamics can be analysed and interpreted.

2 Stepwise eigenvalue analysis of system interconnection

In order to understand and classify the impact of interconnecting two systems on the small-signal dynamics, additional intermediate steps can be introduced in the transition from two disconnected systems to a single interconnected system. This subdivision allows for attributing the overall change in small-signal dynamics to the different implications associated with the interconnection. It should be noted that the presented steps are introduced in a mathematical perspective to gain more insight and are not corresponding to any physical sequence of interconnection.

2.1 Definition of incremental steps for analysis of system interconnection

The connection of two subsystems can be analysed by consecutively evaluating the following proposed steps:

1. The starting point for the analysis should be a reference case for the initial configuration before the interconnection. If relevant, the added system can also be studied in its initial steady-state conditions.
2. The second step accounts for variations in the parameters of the individual subsystems implied by the interconnection. For example, control parameters can be updated to reflect the retuning of the controllers in the two separate subsystems to accommodate the interconnection. This step also includes updates of equivalent electrical parameters in case the electrical interconnection implies parallel or series connection of equivalent resistances, inductances or capacitances. Note that the two subsystems are still analysed as separate systems.
3. The steady-state operating point can change due to the interconnection of the two initially separate subsystems. For systems containing nonlinearities, this implies a change of the linearization point. The third steps assumes two subsystems as in the second step but operating in the steady state conditions of the interconnected system.
4. As a last step, the eigenvalues of the interconnected system are evaluated. The difference in eigenvalues compared to the previous step will identify the change of eigenvalue locations and stability properties that are caused by the interactions between the two subsystems in the interconnected system.

By analysing the interconnection of systems according to these four steps, the change of small-signal dynamics due to the interconnection can be classified. Moreover, the last step separates the effects of dynamic interactions between the subsystems from those related to changes in the system parameters or steady state operating conditions.

2.2 Interpretation of the defined steps

In the following, it is assumed that a dynamic system can be represented on linearized time-invariant state-space form [7]:

$$\Delta\dot{\mathbf{x}} = \mathbf{A}\left(\mathbf{x}_0\right)\cdot\Delta\mathbf{x} + \mathbf{B}\left(\mathbf{x}_0\right)\cdot\Delta\mathbf{u} \qquad (1)$$

The mathematical expression of the four presented steps for analysing the interconnection of two subsystems can be summarized as shown in Fig. 1. The first step corresponds to the analysis of the two systems, S1, and S2, in the disconnected state, denoted by a superscript 'D' for the **A**-matrices. Since the systems are independent, they can be directly assembled into a linearized state-space model, at the linearization point $\mathbf{x}_0^{\mathrm{D}}$, and have a block-diagonal form when analysed together. Thus, the eigenvalues of the two systems can be calculated as:

$$eig\left(\mathbf{A}_1\right) = \left[\, eig\left(\mathbf{A}_{\mathrm{S1}}^{\mathrm{D}}\left(x_0^{\mathrm{D}}\right)\right)^T \quad eig\left(\mathbf{A}_{\mathrm{S2}}^{\mathrm{D}}\left(x_0^{\mathrm{D}}\right)\right)^T \,\right]^T \qquad (2)$$

In the second step, superscript 'C' for the A-matrices indicates an update of system parameters corresponding the configuration of the interconnected system. However, in this step the A-matrices are still established independently for the two separate systems at their individual operating points. In the third step, the A-matrices are established for the steady-state operating conditions $\mathbf{x}_0^{\mathrm{C}}$ of the interconnected system, resulting in $\mathbf{A}^{\mathrm{C}}(\mathbf{x}_0^{\mathrm{C}})$. Thus, all parameters and operating conditions will be as in the interconnected system, but the eigenvalues for the two systems are still independent and can be calculated according to (2).

The last step of the interconnection analysis is to establish the overall **A**-matrix for the entire system. This is obtained by including the off-diagonal submatrices **Γ** and **Θ**, which originally are terms from the B-matrices of the independent

This is the accepted version of a paper published in 13th IET International Conference on AC and DC Power Transmission - ACDC 2017
DOI: 10.1049/cp.2017.0050

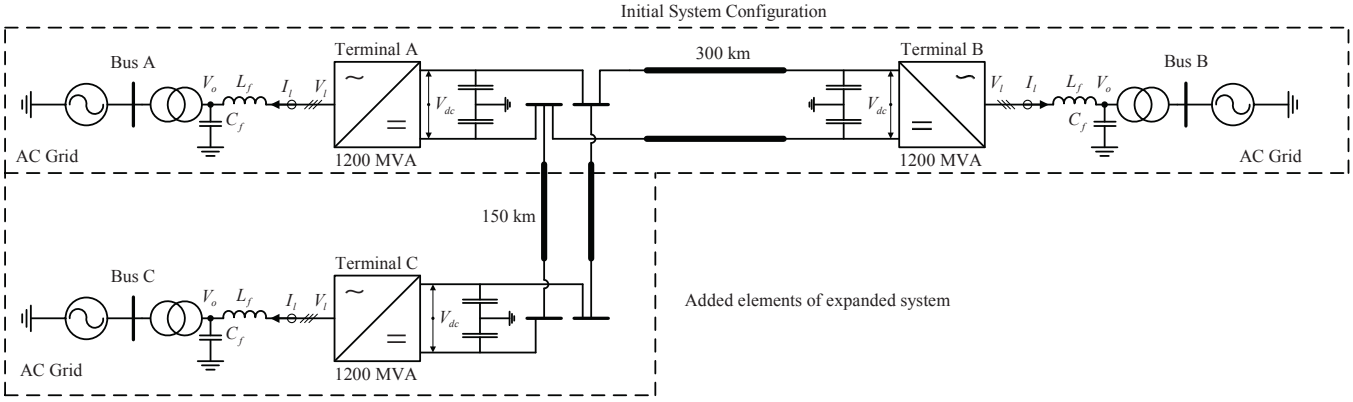

Fig. 2. Overview of investigated VSC-HVDC system, considering the expansion from a P2P scheme to a 3T HVDC grid.

systems that are associated with state-variables of the interconnected system. Thus, the introduction of these off-diagonal submatrices will 'connect' state variables of the two systems, and by that influence the eigenvalues of the A-matrix for the interconnected system. However, if the inputs of a subsystem do not depend only on the states of the other subsystems, but also on states of the subsystem itself, the diagonal block matrixes must also be modified to represent the interconnection. This modification can be defined by introducing the incremental interconnection matrixes **Φ** and **Π** for systems S1 and S2 respectively, as shown Fig. 1. Considering the difference between steps 3 and 4 in Fig. 1, it can be understood that the matrix elements within **Γ**, **Θ, Φ** and **Π** will be responsible for the resulting interactions in the interconnected system.

2.3 Continuous transition between disconnected and connected systems

For further analysing the differences between the eigenvalues in the third and fourth step from Fig. 1, it is possible to define an interconnection variable k for the submatrices **Γ**, **Θ**, **Φ** and **Π** as given by:

$$\mathbf{A}_k = \begin{bmatrix} \mathbf{A}_{S1}^{C}\left(x_0^{C}\right) + k\cdot\boldsymbol{\Phi}\left(\mathbf{x}_0^{C}\right) & k\cdot\boldsymbol{\Gamma}\left(x_0^{C}\right) \\ k\cdot\boldsymbol{\Theta}\left(x_0^{C}\right) & \mathbf{A}_{S2}^{C}\left(x_0^{C}\right) + k\cdot\boldsymbol{\Pi}\left(\mathbf{x}_0^{C}\right) \end{bmatrix}\Bigg|_{k=0\to 1} \quad (3)$$

If the transition from step 3 to step 4 is introduced gradually by varying k between 0 and 1, the impact on the eigenvalue trajectories from disconnected to interconnected conditions (and hence the interactions) can be visualised.

3 Example of stepwise eigenvalue analysis

The proposed approach for stepwise analysis of system interconnection is illustrated with reference to the case of a point-to-point (P2P) HVDC transmission scheme expanded to a 3-terminal (3T) system.

3.1 System configuration

The investigated system configuration is represented in Fig. 2, with the initial P2P transmission scheme shown in the upper part of the figure and the two terminals denoted as A and B. An additional converter terminal denoted as C is connected by a cable to terminal A in the 3T configuration. The P2P system is assumed to operate in steady state with power

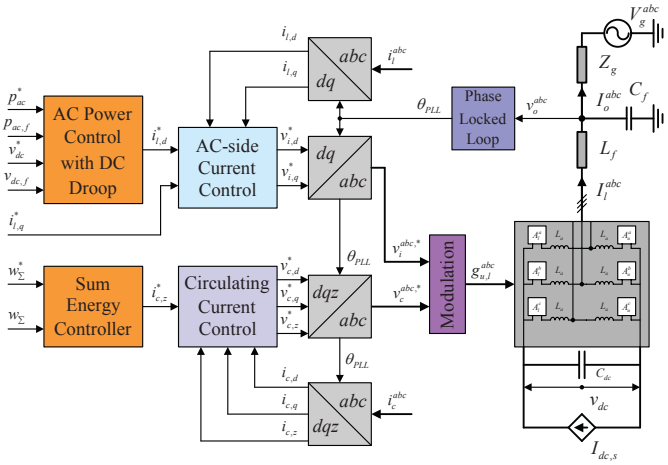

Fig. 3. Overview of MMC HVDC terminal and control system

flowing from terminal A to terminal B ($P_{A,ac}$ = −0.548 pu, $P_{B,ac}$ = 0.540 pu). The 3T system is assumed to operate in steady-state with power flowing from terminal A to terminal B and C ($P_{A,ac}$ = −0.848 pu, $P_{B,ac}$ = 0.274 pu $P_{C,ac}$ = 0.564 pu). The only interconnection variables are the voltage $v_{dc,A}$ at the dc-side of converter station A and the currents at the cable end connected to this terminal.

The converter terminals are assumed to be Modular Multilevel Converters (MMCs) controlled by an ac-side power controller with a dc voltage droop as shown in Fig. 3. Furthermore, the MMC are controlled with a standard decoupled current control, as well as an energy-based control strategy for regulating the internal circulating current and energy sum dynamics [15]. The main parameters of the system are listed in Table I, and the control parameters of the

Parameter	Value	Parameter	Value
Rated voltage $V_{S,LL,RMS}$	220 kV	Filter inductance l_f	0.204 pu
Rated power S_b	1200 MVA	Filter resistance r_{lf}	0.005 pu
Rated angular frequency ω_b	2π*50 Hz	Filter capacitance c_f	0.089 pu
Current controller gains, k_{pc}, k_{ic}	0.26, 2.14	Grid voltage $\hat{v}_g$	1.0 pu
Power controller gains, k_{pp}, k_{ip}	1, 100	PLL Low pass filter, $\omega_{LP,PLL}$	500 rad/s
Power measurement filter, $T_{f,p}$	7.6 ms	PLL gains, $k_{p,PLL}$, $k_{i,PLL}$	0.084, 4.691

Table I Parameters of investigated system configuration

This is the accepted version of a paper published in 13th IET International Conference on AC and DC Power Transmission - ACDC 2017
DOI: 10.1049/cp.2017.0050

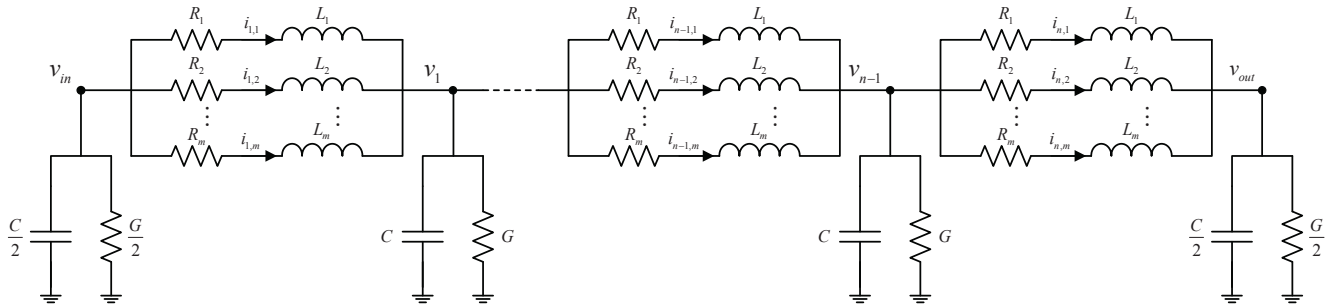

Fig. 4. Frequency-dependent pi-model of HVDC cable

two systems are maintained unaltered after the interconnection (i.e. no retuning of the controllers).

3.2 System modelling

The system is modelled with a non-linear state-space representation and is linearized according to (1). The ac-side electrical circuit and the associated control of each HVDC terminal are modelled according to [16], [17], while a simplified representation of the internal dynamics of the stored energy and the circulating currents of the MMC are modelled according to [18]. The resulting state variables associated with each HVDC terminal are given by (4). The electrical variables are defined in Fig. 3, while $\boldsymbol{\gamma}$ represents integral states of the ac-side current controllers and $\boldsymbol{\varphi}$ is an internal variable associated with an algorithm for damping ac-side oscillations [17]. All state variables with subscript 'PLL' are related to the Phase Locked Loop and further explained in [17]. The states $v_{dc,f}$ and $p_{ac,m}$ represent filtered measurements of the dc voltage and ac-side power respectively, while ρ is a state linked to the integral term of the ac-side power controller. The zero sequence circulating current of the MMC, responsible for the active power exchange with the dc-terminals, is represented by $i_{c,z}$ and the total stored energy in the MMC is represented by w_{Σ}, while ξ_z and k_{Σ} are the states of the associated PI-controllers [18].

The two cables connecting the converter terminals in Fig. 2 are modelled with a frequency-dependent pi-equivalent model according to [19], as shown in Fig. 4. The state variables in this cable model are defined on general form by (5). For sake of simplicity a model with m = 3 parallel branches and n = 4 pi-sections is applied for both cables despite their different length.

Based on the equations presented in [17], [18] and [19], the state-space model of the overall system is established. The corresponding states, and their order as assumed in the following analysis are defined by (6).

3.3 Eigenvalue calculation for the interconnection steps

As a starting point, the eigenvalues of the P2P configuration are shown in Fig. 5 a), while the eigenvalues of the added terminal are shown in Fig. 5 b). An overview of all eigenvalues for the interconnected system is shown in Fig. 5 c). Most of the eigenvalues for the interconnected system are located in close proximity to the combined set of eigenvalues of the two separate subsystems. This corresponds to the interconnected system exhibiting dynamics that resemble those of its components. Indeed, Fig. 5 a), b) and c) illustrate the results usually obtained from the traditional approach of analysing a system before and after interconnection. However, it is relatively difficult to interpret the results and identify the causes of the differences between the modes in the two separated subsystems and the interconnected systems.

In contrast, two enlarged views showing the eigenvalues calculated from a stepwise analysis of the interconnection according to section 2 are presented in Fig. 6. The eigenvalues calculated in step 1 for the P2P system and in step 4 for the interconnected 3T system are denoted as "P2P" and "3T", respectively. Furthermore, the eigenvalues of the intermediate step 2 and 3 are denoted as "P2P^{C}" and "3T^{D}" respectively. The differences in the eigenvalues between step 1 and the step 2 indicate the influence of the equivalent cable capacitance on some of the oscillatory modes that according to the results in [14] are expected to be mainly associated with the cables. The figure also shows that these eigenvalues remain almost in the same positions when passing from step 2 to step 3, which indicates a negligible influence from the steady state operating conditions and linearization point. This indicates that eigenvalues strongly associated with the cable dynamics are not significantly depending on the operating conditions, which should be expected since the cable model itself is linear.

Finally, the modes associated to the dynamic interactions between the two subsystems are revealed by the differences

$$\mathbf{x}_{\mathrm{MMC}} = \begin{bmatrix} v_{o,d} & v_{o,q} & i_{l,d} & i_{l,q} & \gamma_d & \gamma_q & i_{o,d} & i_{o,d} & \varphi_d & \varphi_q & v_{PLL,d} & v_{PLL,q} & \varepsilon_{PLL} & \delta\theta_{PLL} & v_{dc} & v_{dc,f} & \rho & p_{ac,m} & i_{c,z} & w_{\Sigma} & \kappa_{\Sigma} & \xi_z \end{bmatrix} \tag{4}$$

$$\mathbf{x}_{\mathrm{Cable}} = \begin{bmatrix} i_{1,1} & i_{1,1} & \dots & i_{1,n} & v_{c,1} & i_{2,1} & i_{2,2} & \dots v_{c,m-1} & i_{m,1} & i_{m,2} & \dots & i_{m,n} \end{bmatrix}^T \tag{5}$$

$$\mathbf{x}^{\mathrm{C}} = \begin{bmatrix} \underbrace{\mathbf{x}_{\mathrm{MMC1}} \quad \mathbf{x}_{\mathrm{MMC2}} \quad \mathbf{x}_{\mathrm{Cable\ A\text{-}B}}}_{\mathbf{x}_{\mathrm{S1}}} \quad \underbrace{\mathbf{x}_{\mathrm{MMC3}} \quad \mathbf{x}_{\mathrm{Cable\ A\text{-}C}}}_{\mathbf{x}_{\mathrm{S2}}} \end{bmatrix}^T \tag{6}$$

This is the accepted version of a paper published in 13th IET International Conference on AC and DC Power Transmission - ACDC 2017
DOI: 10.1049/cp.2017.0050

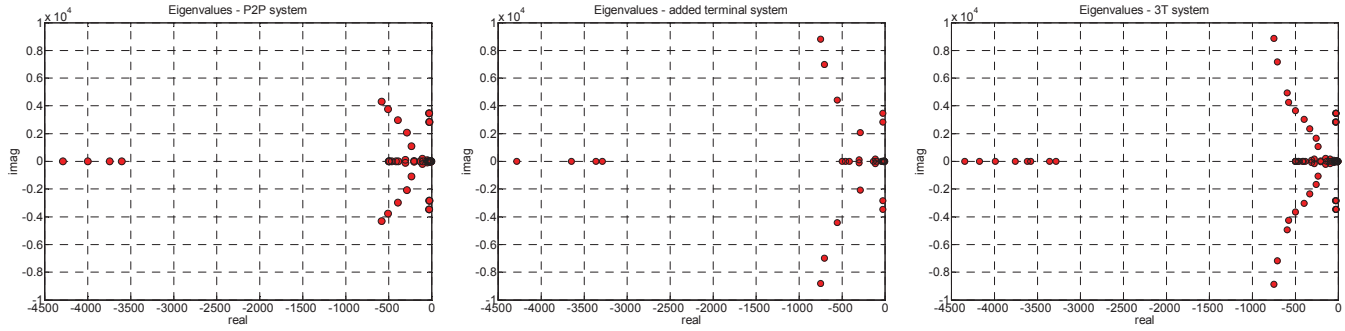

a) System 1 b) System 2 c) System interconnected

Fig. 5. Eigenvalues of the two systems before the interconnection, and of the interconnected system

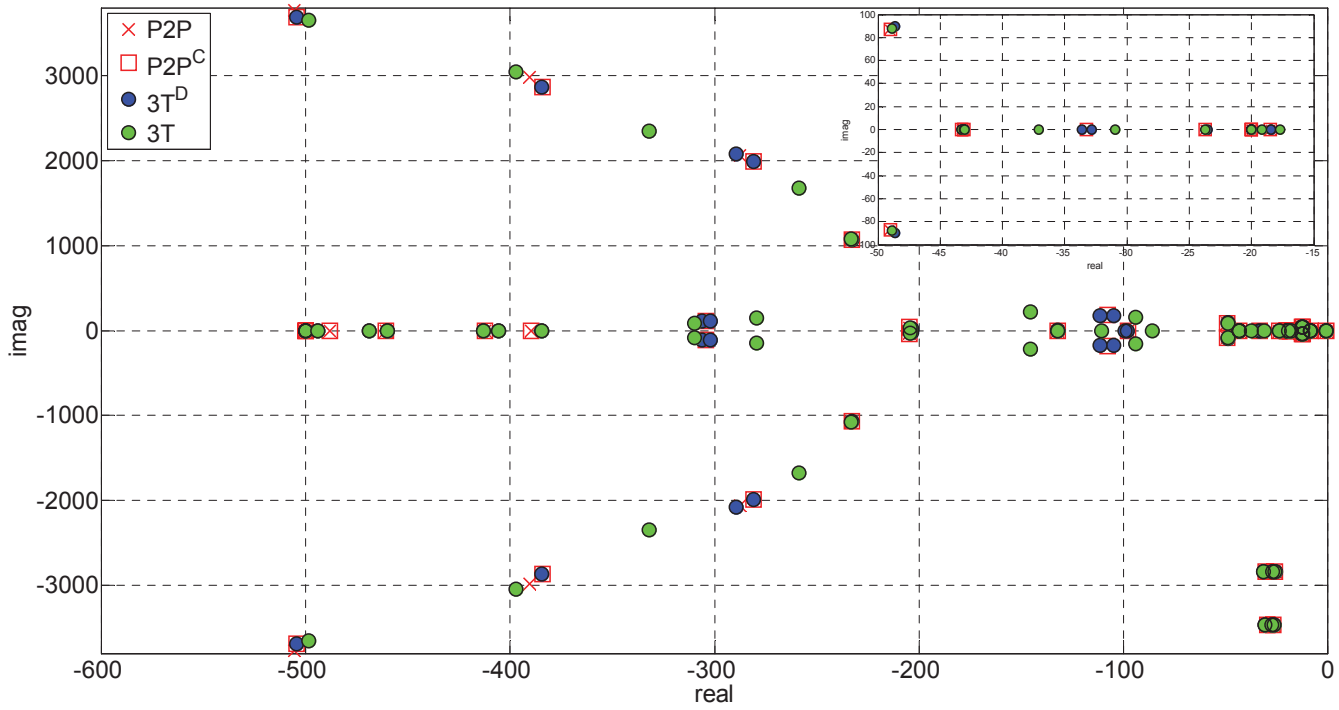

Fig. 6. Partial overview of eigenvalues calculated for the different steps of the interconnection analysis

between the eigenvalues from step 3 and step 4. Indeed, comparing the eigenvalues denoted as "3T^{D}" and "3T" in Fig. 6 clearly highlights how some eigenvalues are significantly influenced by the interconnection, while others remain in almost identical positions. In particular, it can be noticed how two pairs of complex conjugate eigenvalues with real part close to −300 for the "3T^{D}" move noticeably toward the right, or to the left in the final "3T" configuration.

3.4 Matrix elements responsible for interactions

Since the only interconnection between the systems are the capacitor voltage $v_{dc,A}$ at terminal A and the current in the last section of the cable from terminal A to C, the matrixes **Φ** and **Π** from section 2.2 will be zero. Thus, the off-diagonal submatrices **Γ** and **Θ** will determine the interactions in the system. To understand the interconnections in the system, it is relevant to identify the terms included in these submatrices, and. The structure of the resulting A matrix of 3T case and the elements responsible for the interconnection are illustrated in Fig. 7, which is showing the non-zero elements of all the sub-matrixes.

Considering the structure of the 3T system and the states listed in (6), it can be found that the elements of **Γ** and **Θ** that are marked with red in Fig. 7 are given by (7) and (8), respectively. The states that will influence $v_{dc,A}$ due to (7), are given by (9) and represent the three inductors in the parallel branches of the pi section closest to converter terminal A in the cable from A to C. Similarly, only the voltage $v_{dc,A}$ will influence these three currents according to the elements of **Θ** defined in (8).

$$\Gamma_{v_{dc,A},\mathbf{x}_{S2,\text{Cable A-C}}} = \left[\dots \quad -\frac{\omega_b}{c_{eq,A}} \quad -\frac{\omega_b}{c_{eq,A}} \quad -\frac{\omega_b}{c_{eq,A}} \quad \dots \right] \tag{7}$$

$$\Theta_{\mathbf{x}_{S2,\text{Cable A-C}},v_{dc,A}} = \left[\dots \quad \frac{\omega_b}{l_{1_{\text{Cable A-C}}}} \quad \frac{\omega_b}{l_{2_{\text{Cable A-C}}}} \quad \frac{\omega_b}{l_{3_{\text{Cable A-C}}}} \quad \dots \right]^T \tag{8}$$

$$\mathbf{x}_{S2,\text{Cable A-C}} = \left[\dots \quad i_{1,1_{\text{Cable A-C}}} \quad i_{1,2_{\text{Cable A-C}}} \quad i_{1,3_{\text{Cable A-C}}} \quad \dots \right]^T \tag{9}$$

Since these elements can be directly associated with the interactions appearing when connecting the two systems S1

This is the accepted version of a paper published in 13th IET International Conference on AC and DC Power Transmission - ACDC 2017
DOI: 10.1049/cp.2017.0050

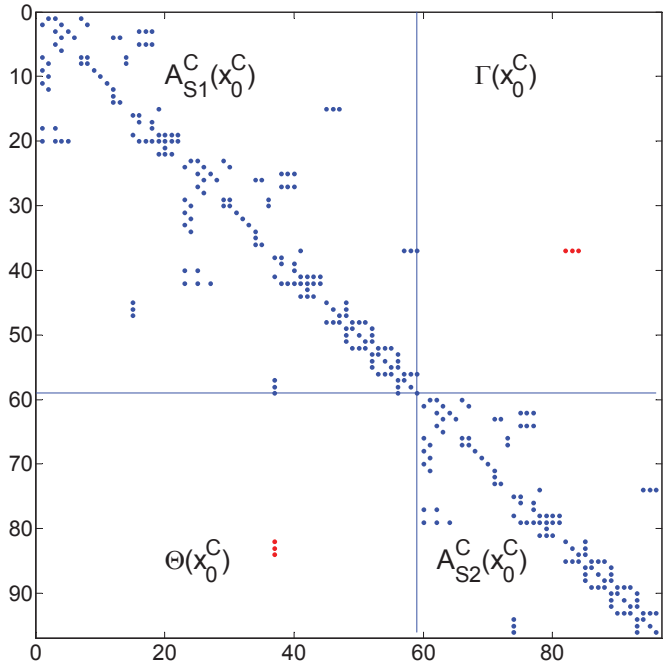

Fig. 7. Overview of non-zero matrix elements for the different sub-matrixes of the interconnected 3T HVDC system

and S2, they can also be used to illustrate the transition between the disconnected and interconnected system configurations, as proposed in section 2.3.

3.5 Interconnection trajectory of eigenvalues

Although the analysis of Fig. 6 reveals the changes in the eigenvalues associated with each step defined in section 2, the results might still be difficult to interpret. For instance, it can be difficult to trace a single eigenvalue before and after the interconnection, especially if the location of the eigenvalue changes significantly and/or moves to a location close to other eigenvalues. However, the variable k defined in (3) can be used to define a smooth transition from the analysis of the disconnected systems (k = 0) to the interconnected system configuration (k = 1) and will provide a simple visualization of how the eigenvalues change. Considering the matrix elements from (7) and (8), it can also be noticed that a value of k = 0 will correspond to equivalent inductances and capacitances at the interconnection approaching infinity, which would imply an effective decoupling of the dynamics in the two systems.

Fig. 8 shows with magenta colour the eigenvalue trajectories when sweeping k in the range from 0 to 1. The initial eigenvalue locations for step 3 and the eigenvalues for the interconnected 3T system corresponding to step 4 are marked respectively with blue and green dots as in Fig. 6. The magenta trajectory illustrates visually how the eigenvalue locations change due to the interconnection of the two subsystems and offers a quantitative measure of the effect of the interactions on the system dynamics. As expected from Fig. 6 several of the complex conjugate eigenvalues with real part around −300 are significantly influenced by the interconnection. Similarly, there are also several eigenvalues

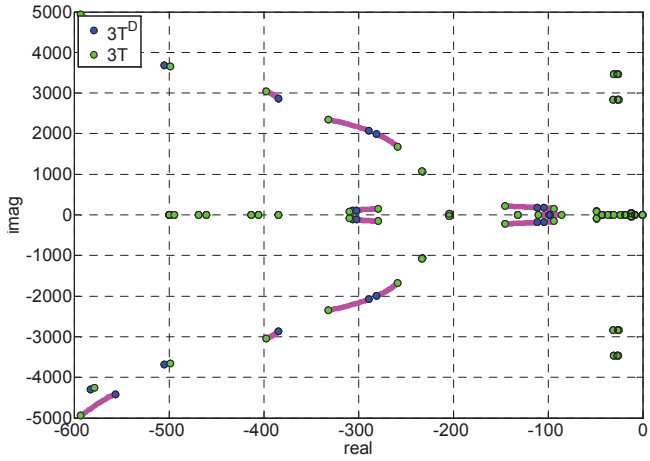

Fig. 8. Eigenvalue trajectory obtained by seamless interconnection of the system according to (3)

with real part around −100 when the systems are not coupled that are noticeably influenced by the interconnection. However, since these eigenvalues were close to each other in Fig. 6, it was not easy to identify how each mode was moving, while this is clearly illustrated by their eigenvalue trajectories in Fig. 8.

4 Comparison to participation factor-based identification of interaction modes

For further demonstrating the relevance and validity of the presented approach, the results from the last step of the analysis are compared to those that can be obtained with the method for identifying system interactions presented in [14].

4.1 Participation factor-based identification of interaction modes

The aggregated participation $\eta_{\alpha,i}$ of a sub-system α in a mode i is defined in the remainder of the study as [14]:

$$\eta_{\alpha,i} = \frac{\|\mathbf{p}_{\alpha,i}\|}{\|\mathbf{p}_i\|} \tag{10}$$

where $\|\mathbf{p}_{\alpha,i}\|$ and $\|\mathbf{p}_i\|$ are the L_1-norms of the vector containing the participation factors associated with the states of sub-system α and the vector containing all the participation factors for mode i, respectively. The relative aggregated participation of a subsystem is defined as:

$$\rho_{\alpha,i} = \frac{\eta_{\alpha,i}}{\sum_{\gamma \in S} \eta_{\gamma,i}} \tag{11}$$

A dynamic mode is then defined as an interaction mode if the relative aggregated participation factors are higher than a threshold χ for at least two subsystems. Thus, for the case of only two interconnected systems S1 and S2, an eigenvalue is considered an interaction mode if $\rho_{S1,i} > \chi$ and $\rho_{S2,i} > \chi$.

4.2 Comparative analysis and discussion

As a reference for comparing the results from the participation factor analysis according to [14] with the result presented in section 3, Fig. 9 a) shows all eigenvalues of the

This is the accepted version of a paper published in 13th IET International Conference on AC and DC Power Transmission - ACDC 2017
DOI: 10.1049/cp.2017.0050

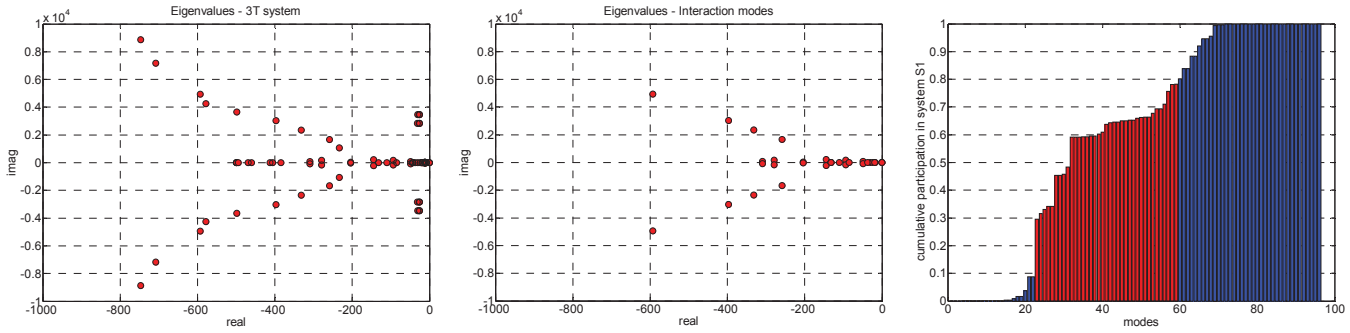

a) Eigenvalues of interconnected system b) Identified interaction modes c) Aggregated participation factors

Fig. 9. Results from participation factor analysis according to [14]

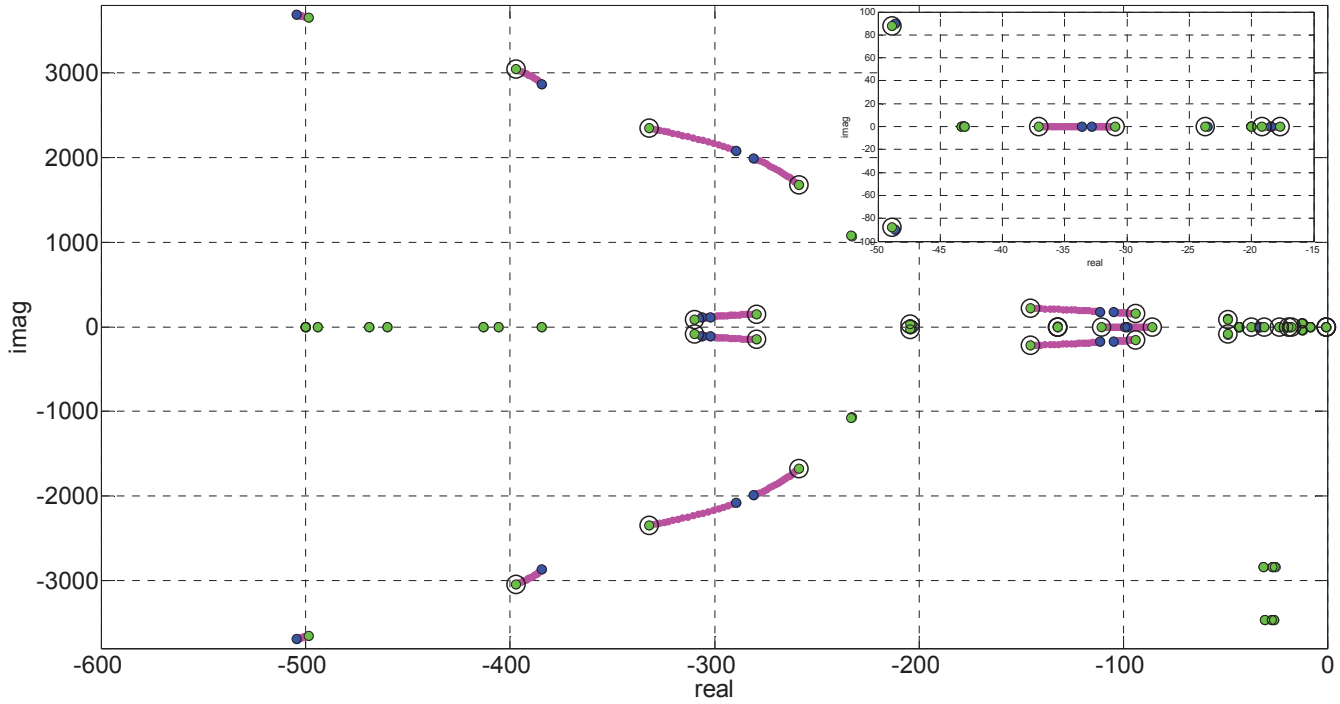

Fig. 10. Comparison between results from participation factor analysis and eigenvalue trajectory for seamless system connection for identifying interactions between the interconnected systems

interconnected system with real part over −1000. Furthermore, Fig. 9 b) shows the interaction modes identified from the aggregated participation factor analysis. An overview of the relative aggregated participation factors with respect to system S1 for all the modes of the interconnected system are shown in Fig. 9 c), when the threshold χ is set to 20 %. In the figure, the interaction modes are displayed as red bars, while the blue bars represent local modes for S1 or S2.

Fig. 10 is showing a combined evaluation of the interconnection sweep from Fig. 8 and the participation factor analysis from Fig. 9 b). The figure shows the same eigenvalue trajectories for the interconnection variable k as in Fig. 8, but in this case, the interaction modes from Fig. 9 b) are marked with a black circle. It can be clearly noticed that all eigenvalues moving significantly due to the interconnection are also interaction modes according to the participation factor analysis. This highlights a strong correlation between the two methods. At a first glance it appears that the method from [14] identifies more interaction modes than those associated with a magenta trace. However, by enlarging the scale of the plot, it can be found that all eigenvalues identified as interaction modes by the participation factor approach are influenced by the interconnection of the system. This may be explained observing that the trajectory of eigenvalues as a function of k indicates also how sensitive the eigenvalue is to the interconnection, while the participation factor analysis identifies only the sharing of the dynamics between more subsystems. From this perspective, the two approaches seem to be compatible and partially complementary. Thus, results from the presented approach can be utilized either independently or to obtain further understanding and insight into results obtained from participation factor analysis.

5 Conclusion

The paper presented a structured approach for analysing the effect on small-signal dynamics from the expansion of a HVDC transmission system. The method is based on a conventional state space representation of the system and on eigenvalue analysis. The transition from the initial system to

This is the accepted version of a paper published in 13th IET International Conference on AC and DC Power Transmission - ACDC 2017
DOI: 10.1049/cp.2017.0050

the expanded system is decomposed in a sequence of steps with a clear mathematical definition, which allows for easily identifying the modes that are influenced by the interconnection. Thus, modes associated with interactions between terminals can be separated from local modes. Moreover, the methodology offers the possibility to distinguish the variations in the dynamic modes due to adjustments of the control parameters and differences in the steady state operating conditions from those more strictly related to the interconnection of the subsystems. A numerical example has been presented, based on the expansion of a point-to-point MMC HVDC connection to a radial three-terminal configuration. Moreover, the methodology has been evaluated against results from participation factor analysis and the interactions modes identified by those two methods have been compared. The results indicate a good agreement between the two procedures.

Acknowledgements

The work of SINTEF Energy Research was supported by the project 'Protection and Fault Handling in Offshore HVDC Grids' (ProOfGrids), financed by the Norwegian Research Council together with industry partners EDF, National Grid, Siemens, Statkraft, Statnett, Statoil and NVE.
Jef Beerten is funded by a postdoctoral research grant from the Research Foundation – Flanders (FWO).

References

[1] N. Flourentzou, V. G. Agelidis, G. D. Demetriades, "VSC-Based HVDC Power Transmission Systems: An Overview," in *IEEE Transactions on Power Electronics*, Vol. 24, No. 3, March 2009, pp. 592-602

[2] J. Peralta, H. Saad, S. Dennetiére, J. Mahseredjian, S. Nguefeu, "Detailed and Averaged Models for a 401-Level MMC-HVDC System," in *IEEE Trans. on Power Delivery*, Vol. 27, No. 3, July 2012, pp. 1501-1508

[3] H. Rao, "Architecture of Nan'ao Multi-terminal VSC-HVDC System and Its Multi-functional Control," in *CSEE Journal of Power and Energy Systems*, Vol. 1, No. 1, March 2015, pp. 9-18

[4] S. Cole, T. K. Vrana, O. B. Fosso, J.-B. Curtis, A.-M. Denis, C.-C. Liu, "A European Supergrid: Present State and Future Challenges," in *Proceedings of the 17th Power System Computation Conference*, PSCC 2011, Stockholm, Sweden, 22-26 August 2011, 7 pp.

[5] T. K. Vrana, R. E. Torres-Olguin, B. Liu, T. M. Hailesellassie, "The North Sea Super Grid – A Technical Perspective, in *Proceedings of the 9th IET International Conference on AC and DC Power Transmission*, ACDC 2010, 19-21 October 2010, London, UK, 5 pp.

[6] D. Van Hertem and M. Ghandhari, "Multi-terminal VSC HVDC for the european supergrid: Obstacles," in *Renewable and Sustainable Energy Review*, vol. 14, no. 9, pp. 3156–3163, December 2010

[7] P. Kundur, "*Power System Stability and Control*," New York, USA, McGraw-Hill, 1993.

[8] G. O. Kalcon, G. P. Adam, O. Anaya-Lara, S. Lo, and K. Uhlen, "Small-signal stability analysis of multi-terminal VSC-based DC transmission systems," *IEEE Transactions on Power Systems* vol. 27, no. 4, November 2012, pp. 1818–1830

[9] N. Chaudhuri, R. Majumder, B. Chaudhuri, and J. Pan, "Stability analysis of VSC MTDC grids connected to multimachine AC systems," *IEEE Trans. on Power Delivery*, vol. 26, no. 4, pp. 2774–2784, October 2011

[10] G. Pinares, M. Bongiorno, "Modeling and Analysis of VSC-based HVDC Systems for DC Network Stability Studies," in *IEEE Transactions on Power Delivery*, vol. 31, no. 2, April 2016, pp. 848-856

[11] M. K. Zadeh, M. Amin, J. A. Suul, M. Molinas, O. B. Fosso, "Small-Signal Stability Study of the Cigré DC Grid Test System with Analysis of Participation Factors and Parameter Sensitivity of Oscillatory Modes," in *Proc. of the 18th Power Systems Computation Conf.*, PSCC 2014, Wrocław, Poland, 18-22 Aug. 2014, 8 pp.

[12] T. K. Vrana, Y. Yang, D. Jovcic, S. Dennetiére, J. Jardini, H. Saad, "The CIGRE B4 DC Grid Test System", CIGRE Electra Magazine, 2013

[13] M. Amin, M. K. Zadeh, J. A. Suul, E. Tedeschi, M. Molinas, O. B. Fosso, "Stability analysis of interconnected AC power systems with multi-terminal DC grids based on the Cigré DC grid test system," in *Proc. of the 3rd Renewable Power Generation Conf.*, RPG 2014, Naples, Italy, 24-25 September 2014, 6 pp.

[14] J. Beerten, S. D'Arco, J. A. Suul, "Identification and Small-Signal Analysis of Interaction Modes in VSC MTDC Systems," in *IEEE Transactions on Power Delivery*, Vol. 31, No. 2, April 2016, pp. 888-897

[15] J. Beerten, G. Bergna Diaz, Salvatore D'Arco, Jon Are Suul, "Comparison of Small-Signal Dynamics in MMC and Two-Level VSC HVDC Transmission Schemes," in *Proc. of the 4th IEEE Int. Energy Conf.*, ENERGYCON 2016, Leuven, Belgium, 4-8 April 2016, 6 pp.

[16] N. Kroutikova, C. Hernandez-Aramburo, and T. Green, "State-space model of grid-connected inverters under current control mode," *IET Electric Power Applications*, vol. 1, no. 3, pp. 329–338, May 2007.

[17] S. D'Arco, J. A. Suul, M. Molinas, "Implementation and Analysis of a Control Scheme for Damping of Oscillations in VSC-based HVDC Grids," in *Proc. of the 16th International Power Electronics and Motion Control Conference and Exposition*, PEMC 2014, Antalya, Turkey, 21-24 September 2014, pp. 586-593

[18] G. Bergna Diaz, J. Suul, and S. D'Arco, "Small-signal state-space modeling of modular multilevel converters for system stability analysis," in *Proc. of the IEEE Energy Conversion Congress and Exposition*, ECCE 2015, Montreal, Québec, Canada, Sep. 20-24, 2015, pp. 5822–5829

[19] J. Beerten, S. D'Arco, J. A. Suul, "Frequency-Dependent Cable Modelling for Small-Signal Stability Analysis of VSC HVDC Systems," in *IET Generation Transmission & Distribution*, Vol. 10, No. 6, April 2016, pp. 1370-1381

This is the accepted version of a paper published in 13th IET International Conference on AC and DC Power Transmission - ACDC 2017
DOI: 10.1049/cp.2017.0050